[1]Chuanfang Zhao*

[2]Huihao Xie

Effect of K and Al Co-Doping on Na3V2 (PO4) 2F3 Cathode Materials

Journal of Electrical Systems

Abstract: - Over the past few decades, sodium-ion batteries have gained recognition as a promising alternative to lithium-ion batteries due to their advantages of abundance, affordability, and high-power energy storage. As of now, cathode materials have emerged as the primary limiting factor in sodium-ion battery performance, considering safety, cost, cycle life, and energy density. Research in this field has mainly concentrated on layered transition metal oxides, polyanionic compounds, and hard carbon anodes as potential cathode materials for sodium-ion batteries. However, many of these materials suffer from drawbacks such as structural distortion and cyclic instability, which will restrict their practical use in sodium-ion batteries.

To address the issues of low capacity in the Na3V2(PO4)2F3 cathode material for sodium-ion batteries and the degradation of lifespan due to structural changes during charging and discharging, this paper introduces a method using the emulsion gel technique to prepare Na3V2(PO4)2F3 cathode materials doped with K at the Na sites and Al at the V sites. This method combines emulsion gelation, freeze-drying, and high-temperature calcination to synthesize the doped cathode materials. The incorporation of K ions in the material enlarges the crystal channels, enabling increased ion storage and thereby enhancing the battery's capacity. Moreover, the inclusion of Al ions preserves the material's layered structure throughout the charging and discharging process, stabilizing the crystal channel structure for the movement of electrons and ions, ultimately enhancing both the battery's capacity and charging efficiency. The cathode material Na3V2(PO4)2F3 in this scheme can achieve stable and reversible charging and discharging across a wider working voltage range, exhibiting high specific capacity and excellent rate performance. The preparation method in this scheme is straightforward and easy to follow, facilitating an increase in production rate and a reduction in production costs while maintaining high performance.

Keywords: Sodium ion battery, Na3V2(PO4)2F3, Doping modification, Latex gel meth.

1.INTRODUCTION

At present, issues such as global warming have attracted widespread attention, and the development of clean energy has been identified as an effective solution. Against this backdrop, lithium-ion batteries (LIBs) have garnered widespread attention for nearly three decades, owing to their high energy and power densities, exceptional cycling performance, and environmental friendliness. However, the scarcity of lithium resources has led to high costs for LIBs, making the search for suitable alternatives critical[1 2 3 4].

Sodium and lithium, both belonging to the same main group, display similar chemical properties and are abundantly found on Earth. This positions sodium-ion batteries (SIBs) as the primary candidate to replace LIBs in energy storage. Additionally, sodium ions, having a larger radius compared to lithium ions, exhibit reduced polarization and solvation energy in liquid electrolyte solvents. This results in improved ion conductivity, more stable solid electrolyte interfaces, decreased dendrite formation, and the ability to use safer solvents, ultimately

[1] College of Materials and Energy of Guangdong University of Technology Guangzhou 510006, Guangdong, China.Email: zhaochuanfang0216@163.com

[2]School of management of Guangdong University of Technology Guangzhou 510520, Guangdong, China.
on-line : journal.esrgroups.org

leading to significantly enhanced safety performance. Although facing technological challenges like cycle life and battery weight, SIBs, with their immense development potential, have garnered extensive research interest and shown promising prospects in the energy storage sector.

SIBs, as an emerging energy storage technology, exhibit several limitations. Their low energy density restricts their use in applications demanding high energy density, and their relatively short cycle life predisposes them to capacity fade and cycling stability issues. These issues may be influenced by structural changes in the cathode material, dissolution and electrolyte deactivation. Owing to the substantially larger size of sodium ions, charging is slower, impacting both the efficiency and speed of battery charging. SIBs typically weigh more than LIBs, which could potentially restrict their adoption in certain applications.

Currently, the primary cathode materials for sodium-ion batteries (SIBs) comprise layered transition metal oxides, polyanionic compounds, Prussian blue and its derivatives, as well as organic compounds. Achieving high-performance SIBs and developing cathode materials with high energy density, exceptional rate capability, and stable cycling performance are essential for meeting the urgent demands of practical applications.

A low-cost, high-performance, and cycle-stable polyanionic $Na_3V_2(PO_4)_2F_3$ (NVPF) cathode material for SIBs, featuring an open NASICON crystal framework, stable sodium-hosting sites, and open three-dimensional ion transport channels, which facilitate rapid sodium ion insertion/deinsertion, thus ensuring good thermal stability. Notably, the $[PO_4]^{3-}$ and F- ion clusters within provide a high operating voltage (approximately 3.95 V) via an "intrinsic induction effect," further enabled high energy output and efficient charge and discharge. These advantages position NVPF as a promising cathode material for SIBs. However, the large ionic radius of Na^+ impedes its deintercalation activity in three-dimensional space5, leading to low Na^+ utilization and making it challenging to achieve the theoretical electrochemical performance. Moreover, a significant amount of Na^+ during the deintercalation process can cause irreversible structural changes to the constructed 3D framework, severely impacting its cycling performance. More importantly, the poor electronic conductivity of $[PO_4]^{3-}$tetrahedral units severely limits their electrochemical performance, especially at high rates.

Therefore, researchers will try methods such as doping impurity ions [17 18] and carbon coating [19 20 21] to improve electrochemical performance, all of which have significant effects. The doping includes Cr^{3+}[22], Y^{3+}[23], Ti^{2+-4+}[24], Mn^{2+}[25], and O^{2-}[26]. Zhu et al. successfully synthesized aluminum doped Na_3V_2-xAlx $(PO_4)_2F_3$ cathode material by the sol-gel method of sodium ion battery.

The Rietveld refinement results of the original $Na_3V_2(PO_4)_2F_3$ and $Na_3V_{1.93}Al_{0.07}(PO_4)_2F_3(PO_4)_2F_3$ confirmed that there was no phase change after Al doping. The optimized $Na_3V_{1.93}Al_{0.07}(PO_4)_2F_3(PO_4)_2F_3$ provides the highest discharge capacity (121.3 $mAhg^{-1}$ at 0.1 C) and maintains 75 % capacity after 400 cycles at 5 C. The rate capability test shows that the rate of $Na_3V_{1.93}Al_{0.07}(PO_4)_2F_3(PO_4)_2F_3$ at 10 °C is as high as 57 $mAhg^{-1}$, which is higher (150 %) than the original NVPF (38 $mAhg^{-1}$). [27]Li et al. examined the impact of K substitution on the crystal structure and electrochemical properties of NVPF.

The results indicated that the incorporation of appropriate K, substituting the Na site in the NVPF crystal structure, effectively widens the ion diffusion path and significantly enhances the electrochemical properties. An impressive cycling performance of 120 $mAhg^{-1}$ was achieved at a low 1 C rate. After 1600 cycles at a discharge rate of 10 C, the discharge capacity remained above 90 $mAhg^{-1}$. Even at a high rate of 50 C, the capacity retention rate of NKVPF@CNT could still maintain a high level of 90% after nearly 6000 cycles.[28]

Therefore, adding K ions to the material can broaden the crystal channels in the material, increase the number of ions that can be stored in the material, and thus improve the capacity of the battery. Moreover, Al ions maintain the layered structure of the material during charging and discharging, stabilized the crystal channel structure of electrons and ions during charging and discharging migration, thereby improving the battery capacity and charging efficiency. This article introduces the simultaneous doping of K ions and Al ions into NVPF positive electrode material, which can achieved stable and reversible charge and discharge in a wider working voltage range, exhibiting high specific capacity and excellent rate performance. The preparation method described in this article is simple and easy to operate, which is conducive to improving the preparation rate and reducing the preparation cost while ensuring high performance.

2. EXPERIMENTAL STEPS

2.1 soliquid-Electrochemical active material of sodium vanadium fluorophosphate ($Na_{2.95}K_{0.05}V_{1.95}Al_{0.05}(PO_4)_2F_3$) was prepared by gel method

Soluble gel method: Synthesis was performed with a target sample volume of 1 g. The quality of the required drug is calculated based on the stoichiometric numbers of $Na_{2.95}K_{0.05}V_{1.95}Al_{0.05}(PO_4)_2F_3$. NaF：KF：$NH_4H_2PO_4$：$NH_4VO_3$：$Al(NO_3)_{3.9}H_2O$ ： $C_6H_8O_7{\cdot}H_2O$ = 2.95 : 0.05 : 2 : 1.95 : 0.05 : 2. Where natrium fluoride takes the stoichiometric number of 0.3 to avoid the loss of sodium and fluorine.

Put ammonium metavanadate and citric acid into a plastic beaker containing a rotor, add about 20 mL of deionized water, put them into a large beaker containing water, and heat them in a water bath with an intelligent magnetic stirrer at a temperature of 80 °C and a stirring speed of about 480 revolutions per minute. Subsequently, sodium fluoride, potassium fluoride, ammonium dihydrogen phosphate, and aluminum nitrate were poured into a beaker and rinsed with a small amount of deionized water. The solution turned dark blue. Keep heating until the sample becomes a gel that no longer flows.

Freeze drying: seal the sample with plastic wrap and poke out many small holes with a needle, then put it into a foam box and pour liquid nitrogen into it for half an hour of quenching. After 30 minutes, remove the beaker and place it in a freeze dryer for 1-2 days of freeze-drying.

Calcination: After thorough grinding, the freeze-dried sample is loaded into a graphite ark. Put it into a tube furnace and calcine it in a pure argon atmosphere. The calcination process is divided into two stages, heating from room temperature to 350 °C at a rate of 1 °C· min^{-1} and holding for 4 hours. After the first stage of insulation is completed, the temperature is raised from 350 °C to 750 °C at a rate of 2 °C· min^{-1}. And keep it at 750 °C for 6 hours until it cools down, then take it out and grind it into a bottle, and store it in a glove box.

2.2 Preparation of the half-batteries

Preparation in advance: after cleaning the glass plate, apply alcohol, put the cut aluminum foil flat on the glass plate, and pull back and forth to eliminate bubbles. After there are no obvious bubbles between the aluminum foil and the glass plate, fix the aluminum foil firmly and set it aside.

Weigh: weigh the resulting active substance according to the ratio of the active substance: acetylene black: PVDF = 8:1:1. The active substance was called 0.12 g, acetylene black 0.015 g, and 0.15 g of glue containing 10 % PVDF.

Mix: mix the three, and add an appropriate amount of N-methyl pyrrolidinone (NMP) as the solvent, use the glass rod to stir, stir evenly, so that there are obvious droplets on the glass rod.

Coating: Apply the sample on the glass plate at the edge of the aluminum foil, scrape the sample from the small beaker spoon and place it on the aluminum foil, so that the sample gathers into strips at the edge of the aluminum foil. Finally, a cleaned 75 μm scraper slowly pushed the sample to the other edge from the edge of the glass plate, allowing the sample to be applied evenly coated on the aluminum foil. The glass plate was subsequently placed in a vacuum drying chamber and dried at 120 °C for 12 h.

Cutting sheet: After the vacuum drying box is cooled, cut the aluminum foil into a diameter of 10 mm with a punching machine. After pressing the tablet by using a tablet press, weigh the electronic balance and record the mass of active material contained in each tablet.

The sodium ion half battery is assembled in the glove box. Take the negative pole shell inverted and load the shrapnel and spacer, place the pole piece in the middle of the spacer with tweezers. Place the flat glass fiber diaphragm on the pole plate, and take the $NaClO_4$ (NC-013) electrolyte drop on the diaphragm with a rubber tip dropper until the diaphragm is completely infiltrated. Then place the torn sodium sheet on the diaphragm and cover with the positive shell. Put in the hydraulic buckle battery seal installed device to seal, dry the electrolyte to get a complete sodium ion half battery, take out the glove box to stand.

2.3 Physical performance characterization

2.3.1 X-ray diffraction (XRD)

The basic principle of XRD is to obtain the diffraction pattern by using the diffraction phenomenon of X-ray are usually produced by accelerated electrons bombarding metal targets. In this experiment, the scanning angle (2 θ) of crystal structure measured by Cu Kα radiation is 10 ° - 80 ° and the scanning speed is 8 °/min.

2.3.2 Scanning electron microscopy (SEM)

The main principle of SEM is to use an electron beam to scan the sample, collect the generated signal, and process it to obtain an image that reflects the surface morphology of the sample, which is used to analyze the microstructure of the substance. Energy dispersive spectroscopy (EDS) is used in conjunction with SEM to qualitatively and analyzed the elemental composition of materials.

2.4 Electrochemical Performance Test

2.4.1 Constant current charge and discharge test

Constant current charge-discharge method is one of the most important methods to study the electrochemical properties of materials. Generally, it can be divided into cycle performance test and rate performance test. The cyclic performance of NVPF and $Na_{2.95}K_{0.05}V_{1.95}Al_{0.05}(PO_4)_2F_3$ was tested under the condition of 300 cycles in the voltage window of 2.0 - 4.5 V and the current density of 0.5 C respectively. The test conditions of magnification performance are as follows: at the current density of 0.2 C, 0.5 C, 1 C , 2 C , 5 C, respectively, 5 cycles and finally at the current density of 0.2 C 5 cycles.

2.4.2 Cyclic Voltammetric Test (CV)

CV is a method used to observe the electrochemical activity of materials. The cyclic voltammetric curve is obtained by scanning at a certain scanning speed within the set interval. There is peak current in the redox

process. By comparing the ratio of peak current and the corresponding potential difference can reflect the reversible degree of the battery. The CV test of the half battery of NVPF and $Na_{2.95}K_{0.05}V_{1.95}Al_{0.05}(PO_4)_2F_3$ has a voltage range of 2.0 - 4.5 V, and the scanning speed increased from 0.1 mVs^{-1} to 0.5 mVs^{-1}.

2.4.3 Electrochemical Impedance Spectroscopy Test (EIS)

EIS, also known as electrochemical impedance spectrum, is to use an electrochemical workstation to apply EIS to the electrode and collect the corresponding impedance changes, so as to obtain the impedance spectrum of the electrode to represent the electrochemical characteristics. The frequency range of this EIS test is $10^{-2} \sim 10^{5}$ HZ, the disturbance voltage amplitude is 10 mV, and the EIS of the sodium ion half battery before charging and discharging is tested.

3. RESULTS AND DISCUSSION

3.1 Analysis of $Na^{2.95}K^{0.05}V^{1.95}Al^{0.05}(PO^4)^2F^3$ material

3.1.1 Analysis of the XRD

In Figure. 1, the XRD spectrum corresponding to the $Na_{2.95}K_{0.05}V_{1.95}Al_{0.05}(PO_4)_2F_3$ material, with a diffraction angle of 10-80 and a sweep speed of 8 min^{-1}. In Figure. 2, the NVPF samples doped with K and Al elements matched well with NVPF (standard card PDF # 89-8485), indicating that NVPF with high purity was prepared in this experiment. At the same time, the position and number of diffraction peaks before and after sodium vanadium fluoride phosphate doping were basically the same, indicating that Al and K doping did not change the crystal structure of sodium vanadium vanadium fluoride phosphate, and maintained the original three-dimensional open structure of sodium vanadium fluoride phosphate together with other atoms. From it, we can see that the main diffraction peaks of the doped sodium vanadium fluoride phosphate are all sharp, which indicates that the crystallinity of the obtained sample is good.

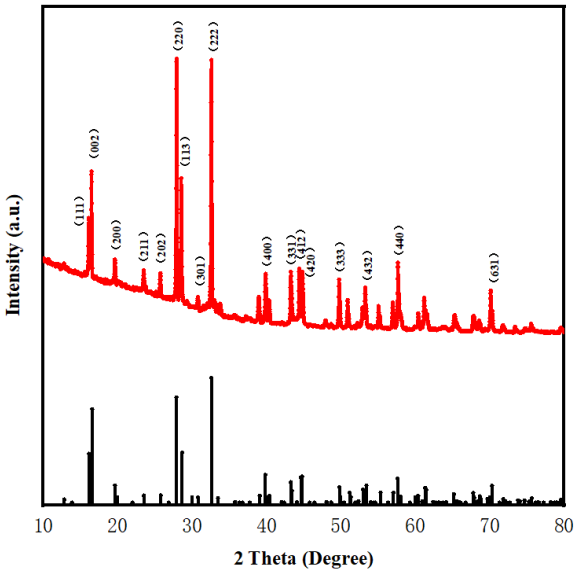

Figure 1. XRD diffraction pattern of $Na_{2.95}K_{0.05}V_{1.95}Al_{0.05}(PO_4)_2F_3$ material

3.1.2 Analysis of the SEM

As shown in Figure. 2, the SEM results also show that the crystallinity of the doped samples is very good because the hexahedral structure can be observed. The particles are very uniform and the average particle size is

between 1-3 nm. At the same time, we can see that K and Al elements are evenly distributed in the crystal and K and Al elements are effectively doped in the sample.

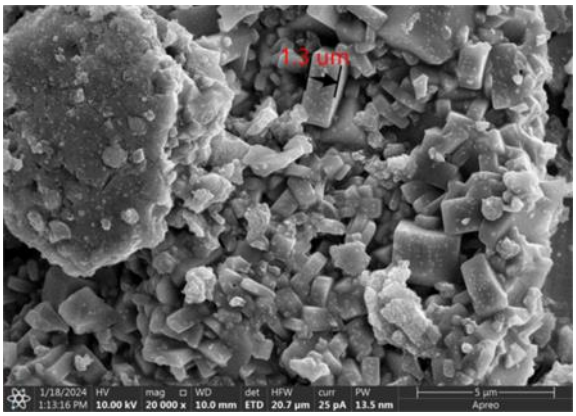

Figure 2. SEM electron micrographs of $Na_{2.95}K_{0.05}V_{1.95}Al_{0.05}(PO_4)_2F_3$ material

3.1.3 Analysis of the EIS

As shown in Figure. 3, the buckle cell assembled with three sample cathode materials at doping concentrations was tested for AC impedance at open circuit voltage. The AC impedance spectrogram of $Na_{2.95}K_{0.05}V_{1.95}Al_{0.05}(PO_4)_2F_3$ is mainly composed of a semicircle and a straight line Where the starting point of the impedance curve is ohmic resistance. The semicircle part represents the high frequency region and represents a series of impedance such as mass transfer resistance,and the linear part represents the low frequency region and represents the Warburg impedance (diffusion impedance) in the battery. The larger the slope of straight line, the larger the diffusion coefficient, the more favorable it is for the diffusion and migration of sodium ions in active substances It can be seen from Figure. 3 that both non-circulating Al and K-doped NVPF samples and pure NVPF samples have the same ohmic resistance. Al and K-doped NVPF samples have higher diffusion coefficients and faster diffusion rates.

After circulation, the resistance of the two samples is obviously different. The resistance of NVPF samples with Al and K samples is significantly lower than that of pure NVPF samples after circulation, but the diffusion rate of NVPF samples with Al and K decreases significantly after circulation, and the diffusion coefficient of the pure samples does not change much.

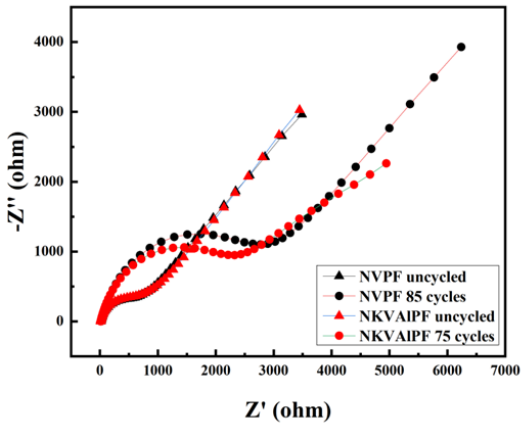

Figure 3. AC impedance spectrum diagram of $Na_{2.95}K_{0.05}V_{1.95}Al_{0.05}(PO_4)_2F_3$ material

3.1.4 Analysis of the CV

As shown in Figure 4, the result of the cyclic voltammetry of the $Na_{2.95}$ $K_{0.05}$ $V_{1.95}$ $Al_{0.05}$ $(PO_4)_2$ F_3 material at different sweep speeds. It is obvious that the peak current of the cyclic Vttammogram of NVPF increases as the scanning speed increases from 0.1 mVs^{-1} to 0.5 mVs^{-1}. At the same time, due to the effect of electrochemical polarization, with the increase of the scanning speed, the oxidation peak of the cyclic voltammetry curve shifts to the positive potential, and the reduction peak continuously shifts to the negative potential, and the degree of offset increases with the increase of the scanning speed.

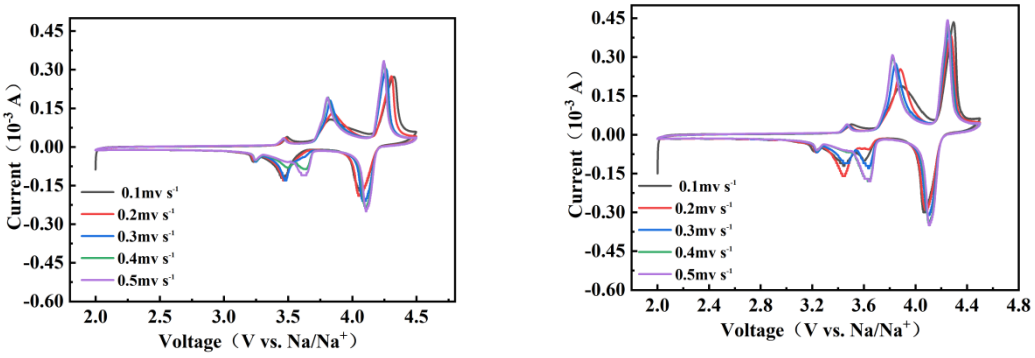

(a) (b)

Figure 4. CV plot of the NVPF material at different sweep speeds：（a）NVPF material；（b）$Na_{2.95}$ $K_{0.05}$ $V_{1.95}$ $Al_{0.05}$ $(PO_4)_2$ F_3 material

As shown in Figure. 4 (a) (b) , with the 0.1 mVs^{-1} sweep in the first circle, we can see that there are three pairs of redox peaks, about 3.3 / 3.4 V, 3.5/3.75 V and 4.1 / 4.2 V. The first two peaks together correspond to the process of Na + exit and embedding from the Na^2 site, while the redox peak at high voltage of 4.1/4.2V corresponds to the process of Na^+ detachment from the Na1 site.

In Figure. 4 (a), we can also see that the splitting of the reduction peak occurs near position 3.5 V, and the partition of the reduction peak also appears around position 3.5 V at multiple sweeps in Figure 4 (b). It is speculated that because the sodium ion concentration near the electrode is too low, the embedding process is controlled by the diffusion step, and the peak division appears. For the better doped samples, the lower sweep also means that the sodium ion embedding can occur better after doping.

By comparing Figure 4 (a) and (b), we can see that figure (a) shows that the pure phase NVPF only has a relatively small redox peak near the position of 3.3 / 3.4 V, which means that the active substance electrochemical activity against this group of voltage positions is not high. With the increase of K and Al doping, the peak potential of 3.3 / 3.4 V will increase. It can be known from the literature that the presence of Al element will induce the appearance of NVPF, namely sodium vanadium phosphate, and the appearance of NVPF improves the redox activity of the sample at 3.3 / 3.4 V, which contributes more capacity to the sample through ion deem bedding. Moreover, it can be seen from comparison that the peak current of the sample after doping is high, indicating that the reductant-oxidant reaction rate on the electrode surface is faster, that is, more substances are involved in the reaction per unit time.

3.1.4 Analysis of constant current charge and discharge results

As shown in Figure. 5, the synthesized charge and discharge curves of sodium vanadium fphosphate at 0.5 C.

All the sodium vanadium aluminum fluorophosphate exhibited a two-stage voltage plateau with a capacity of 3.4 V corresponding to the electrochemical oxidation of vanadium ions from trivalent to tetravalent. At higher voltage, the capacity of sodium vanadium aluminum phosphate exhibits the properties of solid solution, which corresponds to the transition of vanadium ion from tetravalent state to higher valence state.

As shown in figure. 5 (c), the first cycle charge specific capacity of sodium ion battery prepared with undoped NVPF cathode material at 0.5 C is 78.6 mAh/g The coulomb efficiency of 56.9 mAh/g is 97 % after 100 cycles at 0.5 C rate. Moreover, the first cycle charge specific capacity of sodium ion battery prepared by $Na_{2.95}K_{0.05}V_{1.95}Al_{0.05}(PO_4)_2F_3$cathode material at 0.5 C is 93 mAh/g After 100 cycles at 0.5 C, the specific discharge capacity of NVPF was 68.2 mAh/g and the coulomb efficiency was 97 %. Compared with the undoped NVPF, the battery capacity was obviously improved.

The magnification performance of NVPF and $Na_{2.95}K_{0.05}V_{1.95}Al_{0.05}(PO_4)_2F_3$ were tested as shown in Figure. 5 (d). The capacity of NVPF at 0.2 C, 0. 5 C,1 C,2 C,5 C was 84, 75, 67, 59, 48 mAh/g respectively. After high magnification cycle, the capacity of NVPF was still 81 mAh/g at 0.2 C current density. However, $Na_{2.95}K_{0.05}V_{1.95}Al_{0.05}(PO_4)_2F_3$ had a higher battery capacity at 96, 86, 77, 67, 54 and 93 mAh/g at 0.2 C current density after high rate cycling.

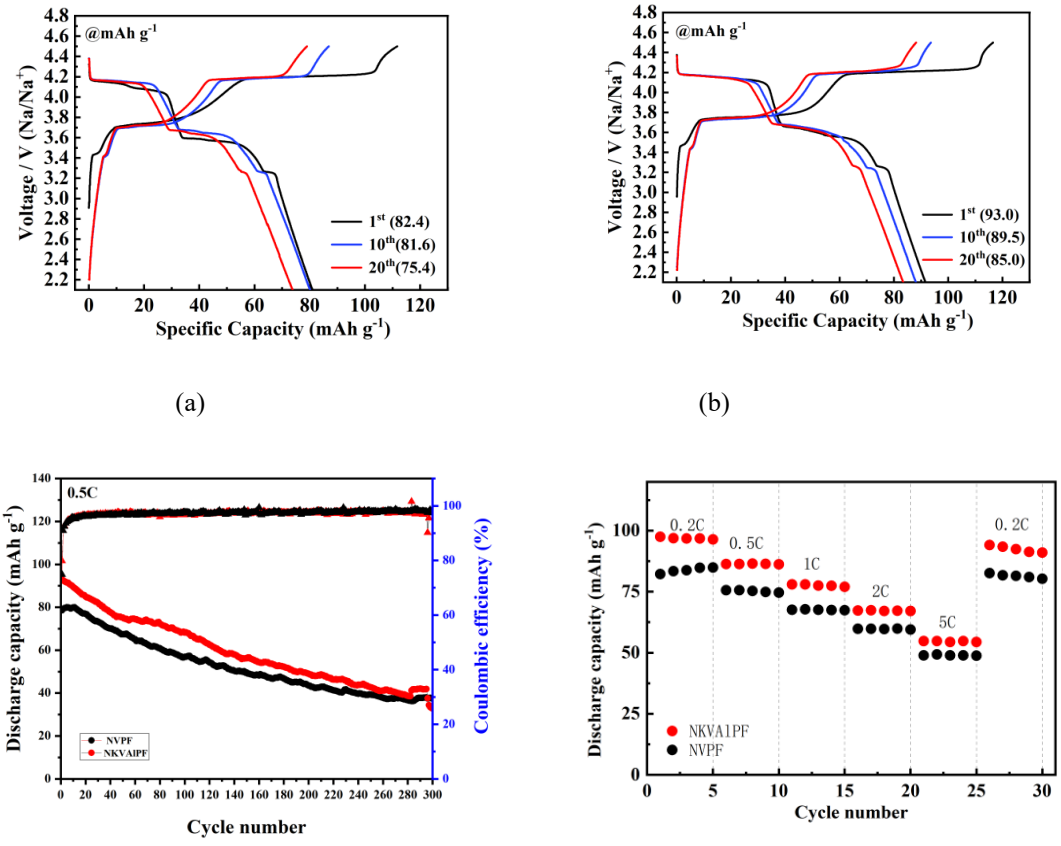

(a) (b)

(c) (d)

Figure 4. Electrochemical performance diagram of the materials:

（a）Charge-discharge curves of NVPF material;

（b）Charge-discharge curves of $Na_{2.95}K_{0.05}V_{1.95}Al_{0.05}(PO_4)_2F_3$ material;

（c）Long Cycle Performance Diagram of NVPF and $Na_{2.95}$ $K_{0.05}$ $V_{1.95}$ $Al_{0.05}$ $(PO_4)_2$ F_3 at 0.5 C ;

（d）Multiplication Performance Diagram of NVPF and $Na_{2.95}$ $K_{0.05}$ $V_{1.95}$ $Al_{0.05}$ $(PO_4)_2$ F_3

4. CONCLUSION

Vanadium sodium fluorophosphate material showed good stability and high battery capacity and rate performance during repeated charge and discharge cycles. This feature is very important to improve the reliability and economy of sodium ion battery. This makes vanadium sodium fluorophosphate material become the focus of research and application, and it is expected to promote the further commercialization of sodium ion battery technology. The incorporation of K and Al into NVPF enhances its capacity and rate capabilities, while expediting the redox reaction at the electrode interface. Nevertheless, the cyclability of this doped NVPF material necessitates further examination. Moving forward, research can delve into optimizing the doping proportions and the synergistic effects between K and Al.

REFERENCES

[1] Wang, Q.; Xu, J.; Zhang, W.; Mao, M.; Wei, Z.; Wang, L.; Cui, C.; Zhu, Y.; Ma, J. Research Progress on Vanadium-Based Cathode Materials for Sodium Ion Batteries. J. Mater. Chem. A 2018, 6 (19), 8815–8838. https://doi.org/10.1039/C8TA01627E.

[2] Xu, G.; Amine, R.; Abouimrane, A.; Che, H.; Dahbi, M.; Ma, Z.; Saadoune, I.; Alami, J.; Mattis, W. L.; Pan, F.; Chen, Z.; Amine, K. Challenges in Developing Electrodes, Electrolytes, and Diagnostics Tools to Understand and Advance Sodium-Ion Batteries. Adv. Energy Mater. 2018, 8 (14), 1702403. https://doi.org/10.1002/aenm.201702403.

[3] Yang, D.-H.; Yao, Z.-Q.; Wu, D.; Zhang, Y.-H.; Zhou, Z.; Bu, X.-H. Structure-Modulated Crystalline Covalent Organic Frameworks as High-Rate Cathodes for Li-Ion Batteries. J. Mater. Chem. A 2016, 4 (47), 18621–18627. https://doi.org/10.1039/C6TA07606H.

[4] Singh, A. N.; Islam, M.; Meena, A.; Faizan, M.; Han, D.; Bathula, C.; Hajibabaei, A.; Anand, R.; Nam, K. Unleashing the Potential of Sodium-Ion Batteries: Current State and Future Directions for Sustainable Energy Storage. Adv. Funct. Mater. 2023, 33 (46), 2304617. https://doi.org/10.1002/adfm.202304617.

[5] Hwang, J.-Y.; Myung, S.-T.; Sun, Y.-K. Sodium-Ion Batteries: Present and Future. Chem. Soc. Rev. 2017, 46 (12), 3529–3614. https://doi.org/10.1039/C6CS00776G.

[6] Aragón, M. J.; Lavela, P.; Ortiz, G. F.; Tirado, J. L. Effect of Iron Substitution in the Electrochemical Performance of Na 3 V 2 (PO 4) 3 as Cathode for Na-Ion Batteries. J. Electrochem. Soc. 2015, 162 (2), A3077–A3083. https://doi.org/10.1149/2.0151502jes.

[7] Yabuuchi, N.; Kubota, K.; Dahbi, M.; Komaba, S. Research Development on Sodium-Ion Batteries. Chem. Rev. 2014, 114 (23), 11636–11682. https://doi.org/10.1021/cr500192f.

[8] Nayak, P. K.; Yang, L.; Brehm, W.; Adelhelm, P. From Lithium-Ion to Sodium-Ion Batteries: Advantages, Challenges, and Surprises. Angew. Chem. Int. Ed. 2018, 57 (1), 102–120. https://doi.org/10.1002/anie.201703772.

[9] Chayambuka, K.; Mulder, G.; Danilov, D. L.; Notten, P. H. L. Sodium-Ion Battery Materials and Electrochemical Properties Reviewed. Adv. Energy Mater. 2018, 8 (16), 1800079. https://doi.org/10.1002/aenm.201800079.

[10] Yang, C.; Xin, S.; Mai, L.; You, Y. Materials Design for High-Safety Sodium-Ion Battery. Adv. Energy Mater. 2021, 11 (2), 2000974. https://doi.org/10.1002/aenm.202000974.

[11] Jin, T.; Li, H.; Zhu, K.; Wang, P.-F.; Liu, P.; Jiao, L. Polyanion-Type Cathode Materials for Sodium-Ion Batteries. Chem. Soc. Rev. 2020, 49 (8), 2342–2377. https://doi.org/10.1039/C9CS00846B.

[12] Du, G.; Pang, H. Recent Advancements in Prussian Blue Analogues: Preparation and Application in Batteries. Energy Storage Mater. 2021, 36, 387–408. https://doi.org/10.1016/j.ensm.2021.01.006.

[13] Aragón, M. J.; Vidal-Abarca, C.; Lavela, P.; Tirado, J. L. Improving the Electrochemical Performance of Titanium Phosphate-Based Electrodes in Sodium Batteries by Lithium Substitution. J. Mater. Chem. A 2013, 1 (44), 13963. https://doi.org/10.1039/c3ta12849k.

[14] Jian, Z.; Hu, Y.-S.; Ji, X.; Chen, W. NASICON-Structured Materials for Energy Storage. Adv. Mater. 2017, 29 (20), 1601925. https://doi.org/10.1002/adma.201601925.

[15] Ong, S. P.; Chevrier, V. L.; Hautier, G.; Jain, A.; Moore, C.; Kim, S.; Ma, X.; Ceder, G. Voltage, Stability and Diffusion Barrier Differences between Sodium-Ion and Lithium-Ion Intercalation Materials. Energy Environ. Sci. 2011, 4 (9), 3680. https://doi.org/10.1039/c1ee01782a.

[16] Zhu, L.; Wang, H.; Sun, D.; Tang, Y.; Wang, H. A Comprehensive Review on the Fabrication, Modification and Applications of Na 3 V 2 (PO 4) 2 F 3 Cathodes. J. Mater. Chem. A 2020, 8 (41), 21387–21407. https://doi.org/10.1039/D0TA07872G.

[17] Du, P.; Mi, K.; Hu, F.; Jiang, X.; Zheng, X. Mn–Doped Hollow Na 3 V 2 O 2 (PO 4) 2 F as a High Performance Cathode Material for Sodium Ion Batteries. Eur. J. Inorg. Chem. 2021, 2021 (13), 1256–1262. https://doi.org/10.1002/ejic.202001159.

[18] Liu, W.; Yi, H.; Zheng, Q.; Li, X.; Zhang, H. Y-Doped Na 3 V 2 (PO 4) 2 F 3 Compounds for Sodium Ion Battery Cathodes: Electrochemical Performance and Analysis of Kinetic Properties. J. Mater. Chem. A 2017, 5 (22), 10928–10935. https://doi.org/10.1039/C7TA03133E.

[19] Pineda-Aguilar, N.; Gallegos-Sánchez, V. J.; Sánchez, E. M.; Torres-González, L. C.; Garza-Tovar, L. L. Aluminum Doped Na3V2(PO4)2F3 via Sol–Gel Pechini Method as a Cathode Material for Lithium Ion Batteries. J. Sol-Gel Sci. Technol. 2017, 83 (2), 405–412. https://doi.org/10.1007/s10971-017-4398-8.

[20] Liu, S.; Cao, X.; Zhang, Y.; Wang, K.; Su, Q.; Chen, J.; He, Q.; Liang, S.; Cao, G.; Pan, A. Carbon Quantum Dot Modified Na 3 V 2 (PO 4) 2 F 3 as a High-Performance Cathode Material for Sodium-Ion Batteries. J. Mater. Chem. A 2020, 8 (36), 18872–18879. https://doi.org/10.1039/D0TA04307A.

[21] Gu, Z.-Y.; Guo, J.-Z.; Sun, Z.-H.; Zhao, X.-X.; Li, W.-H.; Yang, X.; Liang, H.-J.; Zhao, C.-D.; Wu, X.-L. Carbon-Coating-Increased Working Voltage and Energy Density towards an Advanced Na3V2(PO4)2F3@C Cathode in Sodium-Ion Batteries. Sci. Bull. 2020, 65 (9), 702–710. https://doi.org/10.1016/j.scib.2020.01.018.

[22] Yi, X.; Luo, H.; Zhou, Y.; Feng, S.; Wang, J.; Wang, Z.; Duan, J.; Wang, D.; Guo, H.; Yan, G. Effect of Cr3+ Doping on the Electrochemical Performance of Na3V2(PO4)2F3/C Cathode Materials for Sodium Ion Battery. Electrochimica Acta 2023, 437, 141491. https://doi.org/10.1016/j.electacta.2022.141491.

[23] Liu, W.; Yi, H.; Zheng, Q.; Li, X.; Zhang, H. Y-Doped Na 3 V 2 (PO 4) 2 F 3 Compounds for Sodium Ion Battery Cathodes: Electrochemical Performance and Analysis of Kinetic Properties. J. Mater. Chem. A 2017, 5 (22), 10928–10935. https://doi.org/10.1039/C7TA03133E.

[24] Yi, H.; Ling, M.; Xu, W.; Li, X.; Zheng, Q.; Zhang, H. VSC-Doping and VSU-Doping of Na3V2-xTix(PO4)2F3 Compounds for Sodium Ion Battery Cathodes: Analysis of Electrochemical Performance and Kinetic Properties. Nano Energy 2018, 47, 340–352. https://doi.org/10.1016/j.nanoen.2018.02.053.

[25] Zhang, Y.; Guo, S.; Xu, H. Synthesis of Uniform Hierarchical Na 3 V 1.95 Mn 0.05 (PO 4) 2 F 3 @C Hollow Microspheres as a Cathode Material for Sodium-Ion Batteries. J. Mater. Chem. A 2018, 6 (10), 4525–4534. https://doi.org/10.1039/C7TA11105C.

[26] Broux, T.; Bamine, T.; Fauth, F.; Simonelli, L.; Olszewski, W.; Marini, C.; Ménétrier, M.; Carlier, D.; Masquelier, C.; Croguennec, L. Strong Impact of the Oxygen Content in Na3V2(PO4)2F3–yOy (0 ≤ y ≤ 0.5) on Its Structural and Electrochemical Properties. Chem. Mater. 2016, 28 (21), 7683–7692. https://doi.org/10.1021/acs.chemmater.6b02659.

[27] Zhuang, S.-H.; Yang, C.-C.; Zheng, M.; Rengapillai, S.; Marimuthu, S.; Chiang, Y.-S.; Chang, B. K.; Huang, C.-H.; Liu, W.-R. A Combined First Principles and Experimental Study on Al-Doped Na3V2(PO4)2F3 Cathode for Rechargeable Na Batteries. Surf. Coat. Technol. 2022, 434, 128184. https://doi.org/10.1016/j.surfcoat.2022.128184.

[28] Li, L.; Liu, X.; Tang, L.; Liu, H.; Wang, Y.-G. Improved Electrochemical Performance of High Voltage Cathode Na3V2(PO4)2F3 for Na-Ion Batteries through Potassium Doping. J. Alloys Compd. 2019, 790, 203–211. https://doi.org/10.1016/j.jallcom.2019.03.127.

FUNDING

This work was supported by S202311845198

ABOUT THE AUTHOR

Chuanfang Zhao was born in Linfen, Shanxi, China, in 2003. Studying at the School of Materials and Energy of Guangdong University of Technology, majoring in Materials (Innovation Class), with a focus on New Energy Materials and Devices.

E-mail: zhaochuanfang0216@163.com

Huihao Xie was born in Zhuhai, Guangdong, China,in 2003. He currently studying at the School of Management,Guangdong University of Technology. His main research direction is cross-disciplinary research on AI synthetic chemistry.

E-mail: huihao_xie@163.com